THE JOURNAL OF PHYSICAL CHEMISTRY A LETTERS

2007, *111,* 6127−6130
Published on Web 06/20/2007

Interconvertible Side-On- and End-On-Bonded Oxo−Superoxo Titanium Ozonide Complexes

Yu Gong,[†] Mingfei Zhou,*[,†] Shan Xi Tian,[‡] and Jinlong Yang*[,‡]

Department of Chemistry, Shanghai Key Laboratory of Molecular Catalysts and Innovative Materials, Advanced Materials Laboratory, Fudan University, Shanghai 200433, People's Republic of China, and Hefei National Laboratory for Physical Sciences at the Microscale and Department of Chemical Physics, University of Science and Technology of China, Hefei, Anhui 230026, People's Republic of China

Received: May 27, 2007; In Final Form: June 7, 2007

This report presents the preparation and characterization of two interconvertible titanium ozonide complexes using matrix-isolation infrared spectroscopy and density functional theory calculations (B3LYP/6-311+G-(d)). The titanium atoms react with O_2 to form primarily the inserted TiO_2 molecules in solid argon, which further react with O_2 to form OTi(η^2-O_2)(η^2-O_3) via a weakly bonded $TiO_2(O_2)_2$ intermediate. The OTi(η^2-O_2)(η^2-O_3) complex is characterized as $[(TiO)^{2+}(O_2^-)(O_3^-)]$, that is, a side-on-bonded oxo−superoxo titanium ozonide complex. The side-on-bonded complex rearranges to a less stable end-on-bonded OTi(η^2-O_2)(η^1-O_3) isomer under 532 nm laser irradiation, while the reverse reaction (end-on to side-on) proceeds upon sample annealing.

Ozone is widely used as an oxidant in the treatment of water and oxidation of organic and inorganic compounds because of its powerful oxidative ability and low reaction temperature with no side products apart from O_2. The ozonation process can be effectively enhanced by transition metals either in solution or on catalytic supports.[1] Transition metal ozonide complexes can serve as ideal models in understanding the mechanism of ozonation in the oxidation reactions at a molecular level. Due to the extraordinary oxidizing capability of ozone, metal ozonide complexes have not been known so far except for the alkali and alkaline earth metal ozonide complexes, which have been prepared and characterized by X-ray diffraction and matrix-isolation infrared and Raman spectroscopy.[2,3] Recent theoretical investigation has offered some suggestions for stabilizing transition metal complexes of cyclic and open ozone.[4]

Here we report a joint experimental and theoretical study of two titanium ozonide complexes, OTi(η^2-O_2)(η^2-O_3) and OTi(η^2-O_2)(η^1-O_3), which were produced via the reactions of titanium atoms with oxygen in solid argon. Their geometric structures and chemical bonding were investigated via matrix-isolation infrared absorption spectroscopy and density functional theory (DFT) calculations. The two ozonide complexes are interconvertible; that is, formation of end-on-bonded OTi(η^2-O_2)(η^1-O_3) is accompanied by the demise of side-on-bonded OTi(η^2-O_2)(η^2-O_3) under visible (532 nm) light irradiation and vice versa upon annealing.

The above-mentioned species were prepared by co-deposition of laser-evaporated titanium atoms with O_2/Ar mixtures onto a CsI window at 6 K followed by sample annealing and laser irradiation as described previously.[5] Infrared spectra were recorded on a Bruker IFS66V spectrometer at 0.5 cm^{-1} resolution using a liquid-nitrogen-cooled mercury cadmium telluride (MCT) detector. Experiments with high O_2 concentration (0.5−2.0%) and low laser energy (6−8 mJ/pulse) are of interest here. The IR spectra in the selected regions with 0.5% O_2 are shown in Figure 1 with the product absorptions listed in Table 1. In addition to the previously identified TiO, TiO_2,[6] and Ti_2O_4[7] absorptions as well as the known O_3 and O_4^- absorptions,[8] new product absorptions were produced, which can be classified into three groups (labeled as **1**, **2**, and **3** in Figure 1) based on their annealing and photochemical behavior. The absorptions at 938.9 and 908.8 cm^{-1} (**1**) increased together on sample annealing to 35 K but disappeared upon sample annealing to 40 K, during which the 1131.8, 1022.4, 999.8, 806.3, 686.8, and 561.4 cm^{-1} absorptions (**2**) were produced. Visible light (532 nm) irradiation bleached group **2** absorptions with the production of group **3** absorptions at 1341.2, 1117.6, 993.4, 679.8, 554.2, and 516.7 cm^{-1}. Subsequent sample annealing to 35 K destroyed group **3** absorptions and reproduced group **2** absorptions.

Isotopic samples ($^{18}O_2$, $^{16}O_2 + {}^{18}O_2$, and $^{16}O_2 + {}^{16}O^{18}O + {}^{18}O_2$) were employed for product identification based on isotopic shifts and absorption splitting. The 938.9 and 908.8 cm^{-1} absorptions (**1**) exhibited isotopic $^{16}O/^{18}O$ ratios (Table S1 of the Supporting Information) that are characteristic of symmetric and antisymmetric OTiO stretching vibrations. These absorptions are tentatively assigned to the $TiO_2(O_2)_2$ complex. The band positions are only slightly red-shifted (7.9 and 8.2 cm^{-1}) from those of TiO_2 isolated in solid argon,[6] indicating that the interactions between the TiO_2 and the O_2 fragments are very weak.

The absorptions at 1131.8, 1022.4, 999.8, 806.3, 686.8, and 561.4 cm^{-1} (**2**) are assigned to an OTi(η^2-O_2)(η^2-O_3) complex. The band position and $^{16}O/^{18}O$ isotopic frequency ratio of 1.0464

* Authors to whom correspondence should be addressed. E-mail: mfzhou@fudan.edu.cn; jlyang@ustc.edu.cn.
[†] Fudan University.
[‡] University of Science and Technology of China.

10.1021/jp074097o CCC: $37.00

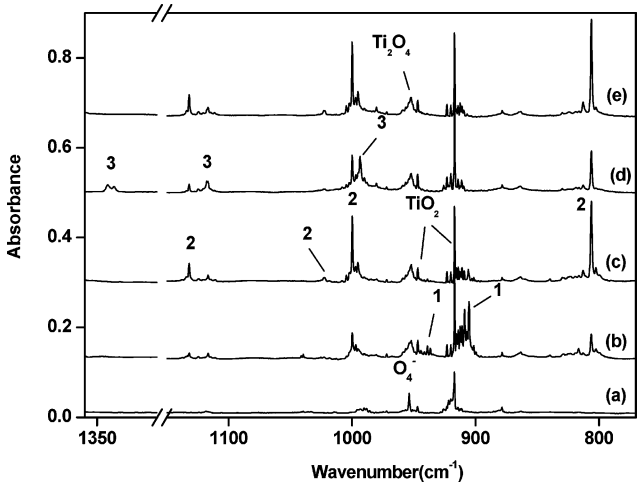

Figure 1. Infrared spectra in the 1360−1300 and 1150−770 cm^{-1} regions from co-deposition of laser-evaporated titanium atoms with 0.5% O_2 in argon: (a) 1 h of sample deposition at 6 K, (b) after 35 K annealing, (c) after 40 K annealing, (d) after 15 min of 532 nm irradiation, and (e) after 35 K annealing.

TABLE 1: Observed and Calculated Vibrational Frequencies (cm^{-1}) and Isotopic Frequency Ratios of the OTi(η^2-O_2)(η^2-O_3) and OTi(η^2-O_2)(η^1-O_3) Complexes

		frequency		$^{16}O/^{18}O$	
molecule	mode[a]	calcd	obsd	calcd	obsd
OTi(η^2-O_2)(η^2-O_3) (^{3}A)	O_2 stretch	1200.7	1131.8	1.0607	1.0633
	O_3 symmetric stretch	1071.6	1022.4	1.0539	1.0557
	Ti≡O stretch	1087.6	999.8	1.0507	1.0464
	O_3 asymmetric stretch	843.9	806.3	1.0602	1.0586
	O_3 bending	699.0	686.8	1.0580	1.0540
	Ti−O_2 stretch	553.7	561.4	1.0313	1.0305
OTi(η^2-O_2)(η^1-O_3) (^{3}A′)	O_3 stretch (a′)	1370.0	1341.2	1.0607	1.0582
	O_2 stretch (a′)	1192.4	1117.6	1.0607	1.0630
	Ti≡O stretch (a′)	1061.0	993.4	1.0440	1.0435
	O_3 bending (a′)	721.5	679.8	1.0482	1.0460
	Ti−O_2 stretch (a′)	591.5	554.2	1.0434	1.0439
	Ti−O_3 stretch (a′)	507.2	516.7	1.0505	1.0513

[a] Some modes listed are mixed, and only the major component is listed.

imply that the 999.8 cm^{-1} absorption is mainly due to a terminal Ti≡O stretching vibration.[6,9] The 1131.8 cm^{-1} absorption shifted to 1064.3 cm^{-1} with $^{18}O_2$. The band position and isotopic $^{16}O/^{18}O$ ratio are characteristic of the O−O stretching vibration of a superoxo ligand.[10,11] The spectra with the $^{16}O_2 + {}^{18}O_2$ and $^{16}O_2 + {}^{16}O^{18}O + {}^{18}O_2$ mixtures (Figure S2 of the Supporting Information) indicate that one side-on-bonded O_2 subunit is involved in this mode. The 561.4 cm^{-1} absorption is due to the corresponding Ti−O_2 stretching mode. The 806.3 cm^{-1} absorption also exhibits a O−O stretching frequency ratio (Table 1). In the experiment with an equal molecular mixture of $^{16}O_2$ and $^{18}O_2$, four absorptions with about the same IR intensities are observed, while a sextet with approximately 1:2:1:1:2:1 relative intensities is clearly resolved in the experiment with a 1:2:1 mixture of $^{16}O_2 + {}^{16}O^{18}O + {}^{18}O_2$ (Figure S3 of the Supporting Information). These spectral features indicate that the 806.3 cm^{-1} absorption is due to the antisymmetric O−O stretching mode of a side-on-bonded O_3 subunit. The much weaker 1022.4 and 686.8 cm^{-1} absorptions are due to the symmetric O−O stretching and bending modes of the O_3 subunit.

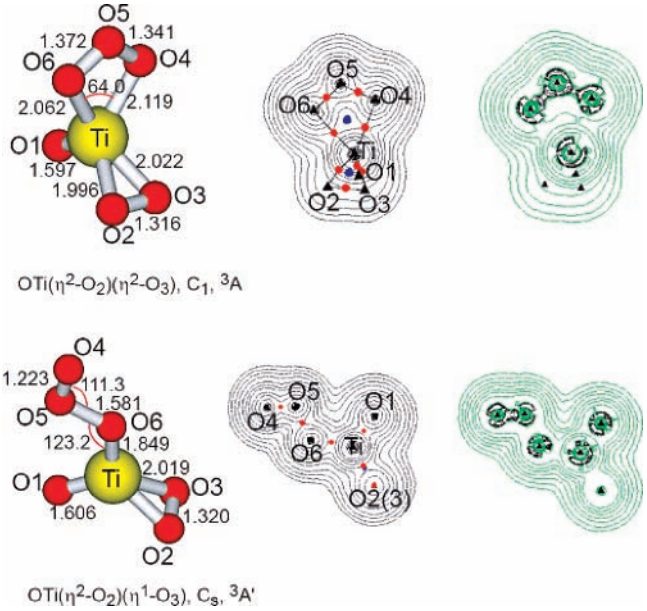

Figure 2. Optimized structures of the OTi(η^2-O_2)(η^2-O_3) and OTi(η^2-O_2)(η^1-O_3) complexes (bond lengths in angstroms, bond angles in degrees) on the left, the electron density ρ contour maps in the middle (black, atomic positions; red, bond critical points; blue, ring critical points), and the density gradient maps $\nabla^2\rho$ on the right (green lines denoting regions of electronic charge connection, and black lines denoting regions of electronic charge depletion). The contours of $\nabla^2\rho$ increase(+)/decrease(−), respectively, from the zero contour in the order of $\pm 2 \times 10^{-n}$, $\pm 4 \times 10^{-n}$, $\pm 8 \times 10^{-n}$, with n- beginning from 3 and decreasing in steps of unity.

The absorptions at 1341.2, 1117.6, 993.4, 679.8, 554.2, and 516.7 cm^{-1} (**3**) appeared under 532 nm laser irradiation at the expense of the OTi(η^2-O_2)(η^2-O_3) absorptions, which suggest that group **3** absorptions belong to a structural isomer of the OTi(η^2-O_2)(η^2-O_3) complex. The isotopic substitution experiments (Figure S4 of the Supporting Information) indicate that the 1117.6 and 554.2 cm^{-1} absorptions are due to the O−O and Ti−O_2 stretching vibrations of a superoxo ligand and the 993.4 cm^{-1} absorption is a terminal Ti≡O stretching mode. These absorptions are only several wavenumbers red-shifted from the corresponding vibrations of the OTi(η^2-O_2)(η^2-O_3) complex, indicating that species **3** also involves an OTi(η^2-O_2) structural unit with the O_3 subunit bonded in a different fashion than in the OTi(η^2-O_2)(η^2-O_3) complex. The 1341.2 cm^{-1} absorption shifted to 1267.4 cm^{-1} with $^{18}O_2$. The band position and isotopic frequency ratio of 1.0582 imply that this absorption is due to an end-on-bonded O−O stretching vibration. Accordingly, group **3** absorptions are assigned to different vibrational modes of an OTi(η^2-O_2)(η^1-O_3) complex (Table 1).

To validate the experimental assignment and to have insights into the structural and bonding nature of the complexes, we carried out DFT calculations at the B3LYP level[12] and natural bond orbital[13] and atoms-in-molecules analyses.[14] Both the side-on- and the end-on-bonded structures were predicted to have a triplet ground state. The singlet states were predicted to lie more than 30 kcal/mol higher. The optimized structures and electron density maps for OTi(η^2-O_2)(η^2-O_3) and OTi(η^2-O_2)(η^1-O_3) are shown in Figure 2. The calculated vibrational frequencies and isotopic frequency ratios (Table 1) are in good agreement with the experimental values, which add strong support to the experimental assignment. For the OTi(η^2-O_2)(η^2-O_3) complex, a C_s structure in which the O_3 subunit and the central Ti atom lie in the same plane that is perpendicular to the molecular plane is considered. This C_s structure is a transition state based on

TABLE 2: Bond Orders and Atoms-in-Molecules Analyses for the OTi(η^2-O_2)(η^2-O_3) and OTi(η^2-O_2)(η^1-O_3) Complexes

	Ti−O1	Ti−O2(3)	Ti−O4(6)	O2−O3	ring (TiO2O3)	ring (TiO4O5O6)
			OTi(η^2-O_2)(η^2-O_3)			
ρ(au)	0.283	0.092 (0.085)	0.069 (0.080)	0.399	0.070	0.035
$\nabla^2\rho$(au)	0.855	0.395 (0.378)	0.292 (0.347)	−0.222	0.512	0.198
bond order	2.752	0.531 (0.530)	0.519 (0.529)	1.510		
			OTi(η^2-O_2)(η^1-O_3)			
ρ(au)	0.276	0.086	0.135[a]	0.394	0.068	
$\nabla^2\rho$(au)	0.854	0.382	0.574[a]	−0.183	0.501	
bond order	2.664	0.632	0.822[a]	1.492		

[a] Only for the Ti−O6 bond.

the presence of a negative calculated frequency. The true minimum is only slightly distorted from the C_s symmetry. The side-on-bonded O_2 fragment has an O−O bond length of 1.316 Å, which falls into the superoxide category.[10] The O_3 fragment also bound in a η^2 side-on fashion with two nearly equivalent Ti−O bond lengths of 2.062 and 2.119 Å, respectively. The experimentally observed antisymmetric O−O stretching vibration of the O_3 subunit is very close to that of the O_3^- anion isolated in solid argon.[15] While the O_2 and O_3 subunits coordinate with the Ti atom by forming weak Ti−O bonds (bond order ≈ 0.5, Table 2), the Ti−O1 bond is strongly covalent-bonded (bond order ≈ 2.8) with a bond length of 1.597 Å. Therefore, the OTi(η^2-O_2)(η^2-O_3) complex can be regarded as a side-on-bonded oxo−superoxo titanium ozonide complex, $[(TiO)^{2+}(O_2^-)(O_3^-)]$, that is, a TiO^{2+} dication coordinated by one O_2^- anion and one O_3^- anion. The natural atomic population calculations also support this conclusion; i.e., Ti is positively charged with 1.613*e*, while the O_2 and O_3 subunits are negatively charged with −0.437*e* and −0.579*e*, respectively. The OTi(η^2-O_2)(η^1-O_3) complex was predicted to have a $^3A'$ ground state with a C_s symmetry. The geometric features of the OTi(η^2-O_2) structural unit in OTi(η^2-O_2)(η^1-O_3) are about the same as those in the OTi(η^2-O_2)(η^1-O_3) isomer. The O_3 fragment lies in the molecular plane and bound in a η^1 end-on fashion with two different O−O bonds. (The terminal one has a bond length of 1.223 Å; another one has a bond length of 1.581 Å.) The complex also can be described as $[(TiO)^{2+}(O_2^-)(O_3^-)]$, an end-on-bonded oxo−superoxo titanium ozonide complex.

The bonding and coordinating features are also shown by the electron distribution contour maps in Figure 2. The red and blue solid circles represent the bond critical points (BCPs) and ring critical points (RCPs). Their related values of electron density ρ (au) and $\nabla^2\rho$ (au) are given in Table 2. In OTi(η^2-O_2)(η^2-O_3), the ρ value (0.069 and 0.080 au) at the BCP between Ti and O4 or O6 is smaller than the others, in line with the weak interaction between Ti and O4 (O6) (i.e., bond order ≈ 0.5). There is no BCP between Ti and O5, but a RCP with $\rho \approx$ 0.035 au exists for the TiO4O5O6 ring. The covalent bonds of the O_3 subunit can clearly be seen from the $\nabla^2\rho$ contour map. Another coordination shows a RCP with $\rho \approx 0.070$ au for the TiO2O3 ring, indicating that the coordination interaction for Ti and O_2 subunit is stronger than that for Ti and O_3 subunit. This suggests that the coordination between Ti and O_3 should more easily be broken if proper energy is provided. The formation of the stable OTi(η^2-O_2)(η^1-O_3) isomer under 532 nm laser irradiation confirms this conjecture. The Ti−O4 bond is broken, whereas the Ti−O6 bond is strengthened ($\rho \approx 0.135$ au at the BCP) in OTi(η^2-O_2)(η^1-O_3).

SCHEME 1

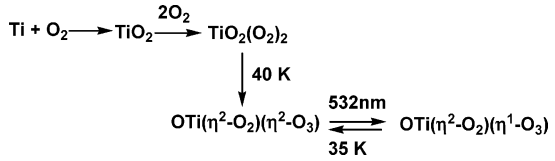

The experimental observations lead us to propose the reactions in Scheme 1.

The titanium atoms react with O_2 to form primarily the inserted TiO_2 molecules in solid argon. Annealing the matrix sample allows the O_2 molecules to diffuse and react with TiO_2 to form the very weakly bonded $TiO_2(O_2)_2$ complex, which further isomerizes to the OTi(η^2-O_2)(η^2-O_3) complex upon sample annealing to around 40 K. The ground state OTi(η^2-O_2)(η^2-O_3) complex was predicted to be 29.0 kcal/mol more stable than $TiO_2 + 2O_2$. The observation of OTi(η^2-O_2)(η^2-O_3) under 40 K annealing suggests that the reaction from the weakly bonded $TiO_2(O_2)_2$ complex to OTi(η^2-O_2)(η^2-O_3) requires very small activation energy. The side-on-bonded OTi(η^2-O_2)(η^2-O_3) rearranges to the end-on-bonded OTi(η^2-O_2)(η^1-O_3) isomer under 532 nm laser irradiation. The experimental observations indicate that the isomerization reactions are reversible; that is, formation of the end-on-bonded OTi(η^2-O_2)(η^1-O_3) isomer is accompanied by demise of the side-on-bonded OTi(η^2-O_2)(η^2-O_3) complex under 532 nm laser irradiation and vice versa upon sample annealing. The side-on-bonded complex was predicted to be 7.3 kcal/mol more stable than the end-on-bonded complex at the B3LYP level of theory. The reaction from side-on to end-on was computed to have a barrier height of 10.5 kcal/mol at the triplet potential energy surface. Experimentally, the side-on to end-on process proceeds only under 532 nm irradiation, during which some excited states may be involved. The TiO molecule has a high density of allowed transitions in the visible region for excitation of the metal monoxide in the OTi(η^2-O_2)(η^2-O_3) complex.[16] The reverse reaction (end-on to side-on) is exothermic and has a much lower barrier (3.2 kcal/mol) and, hence, is able to proceed on sample annealing.

In summary, we have prepared and identified two side-on- and end-on-bonded oxo−superoxo titanium ozonide complexes, which can be interconverted upon irradiation and annealing. These new oxygen-rich transition metal ozonide complexes are potential important intermediates in catalytic oxidation reactions with molecular ozone.

Acknowledgment. This work is supported by NKBRSF (Grant Nos. 2004CB719501 and 2006CB922000) and NNSFC (Grant No. 20433080).

Supporting Information Available: Experimental isotopic frequencies, spectra, and calculated geometries (as Cartesian coordinates) of the aforementioned species. This material is available free of charge via the Internet at http://pubs.acs.org.

References and Notes

(1) For recent reviews, see: (a) Kasprzyk-Hordern, B.; Ziolek, M.; Nawrocki, J. *Appl. Catal., B* **2003**, *46*, 639. (b) Griffith, W. P. *Coord. Chem. Rev.* **2001**, *219−221*, 259. (c) Oyama, S. T. *Catal. Rev.−Sci. Eng.* **2000**, *42*, 279. (d) Legube, B.; Karpel Vel Leitner, N. *Catal. Today* **1999**, *53*, 61.

(2) (a) Klein, W.; Jansen, M. *Z. Naturforsch., B: Chem. Sci.* **2005**, *60*, 426. (b) Klein, W.; Jansen, M. *Z. Anorg. Allg. Chem.* **2000**, *626*, 947. (c) Klein, W.; Armbruster, K.; Jansen, M. *Chem. Commun.* **1998**, 707. (d) Kellersohn, T.; Korber, N.; Jansen, M. *J. Am. Chem. Soc.* **1993**, *115*, 11254. (e) Schnick, W.; Jansen, M. *Z. Anorg. Allg. Chem.* **1986**, *532*, 37.

(3) (a) Andrews, L.; Prochaska, E. S.; Ault, B. S. *J. Chem. Phys.* **1978**, *69*, 556. (b) Spiker, R. C., Jr.; Andrews, L. *J. Chem. Phys.* **1973**, *59*, 1851.

(c) Andrews, L. *J. Am. Chem. Soc.* **1973**, *95*, 4487. (d) Bates, J. B.; Brooker, M. H.; Boyd, G. E. *Chem. Phys. Lett.* **1972**, *16*, 391.

(4) Flemmig, B.; Wolczanski, P. T.; Hoffmann, R. *J. Am. Chem. Soc.* **2005**, *127*, 1278.

(5) (a) Wang, G. J.; Gong, Y.; Chen, M. H.; Zhou, M. F. *J. Am. Chem. Soc.* **2006**, *128*, 5974. (b) Zhou, M. F.; Andrews, L.; Bauschlicher, C. W., Jr. *Chem. Rev.* **2001**, *101*, 1931.

(6) Chertihin, G. V.; Andrews, L. *J. Phys. Chem.* **1995**, *99*, 6356.

(7) Gong, Y.; Zhang, Q. Q.; Zhou, M. F. *J. Phys. Chem. A* **2007**, *111*, 3534.

(8) (a) Chertihin, G. V.; Andrews, L. *J. Chem. Phys.* **1998**, *108*, 6404. (b) Andrews, L.; Spiker, R. C., Jr. *J. Phys. Chem.* **1972**, *76*, 3208.

(9) (a) Miao, L.; Dong, J.; Yu, L.; Zhou, M. F. *J. Phys. Chem. A* **2003**, *107*, 1935. (b) Zhou, M. F.; Zhang, L. N.; Dong, J.; Qin, Q. Z. *J. Am. Chem. Soc.* **2000**, *122*, 10680.

(10) (a) Cramer, C. J.; Tolman, W. B.; Theopold, K. H.; Rheingold, A. L. *Proc. Natl. Acad. Sci. U.S.A.* **2003**, *100*, 3635. (b) Hill, H. A. O.; Tew, D. G. *Comprehensive Coordination Chemistry*; Wilkinson, G.; Gillard, R. D.; McCleverty, J. A., Eds.; Pergamon Press: Oxford, U. K., 1987; Vol. 2, p 315.

(11) (a) Bahlo, J.; Himmel, H. J.; Schnöckel, H. *Angew. Chem., Int. Ed.* **2001**, *40*, 4696. (b) Stösser, G.; Schnöckel, H. *Angew. Chem., Int. Ed.* **2005**, *44*, 4261.

(12) The DFT calculations were performed using the B3LYP method with the 6−311+G(d) basis set: (a) Becke, A. D. *J. Chem. Phys.* **1993**, *98*, 5648. (b) Lee, C.; Yang, W.; Parr, R. G. *Phys. Rev. B* **1988**, *37*, 785. (c) McLean, A. D.; Chandler, G. S. *J. Chem. Phys.* **1980**, *72*, 5639. (d) Krishnan, R.; Binkley, J. S.; Seeger, R.; Pople, J. A. *J. Chem. Phys.* **1980**, *72*, 650. All of these calculations were performed using the Gaussian 03 program: Frisch, M. J.; Trucks, G. W.; Schlegel, H. B.; Scuseria, G. E.; Robb, M. A.; Cheeseman, J. R.; Montgomery, J. A., Jr.; Vreven, T.; Kudin, K. N.; Burant, J. C.; Millam, J. M.; Iyengar, S. S.; Tomasi, J.; Barone, V.; Mennucci, B.; Cossi, M.; Scalmani, G.; Rega, N.; Petersson, G. A.; Nakatsuji, H.; Hada, M.; Ehara, M.; Toyota, K.; Fukuda, R.; Hasegawa, J.; Ishida, M.; Nakajima, T.; Honda, Y.; Kitao, O.; Nakai, H.; Klene, M.; Li, X.; Knox, J. E.; Hratchian, H. P.; Cross, J. B.; Bakken, V.; Adamo, C.; Jaramillo, J.; Gomperts, R.; Stratmann, R. E.; Yazyev, O.; Austin, A. J.; Cammi, R.; Pomelli, C.; Ochterski, J. W.; Ayala, P. Y.; Morokuma, K.; Voth, G. A.; Salvador, P.; Dannenberg, J. J.; Zakrzewski, V. G.; Dapprich, S.; Daniels, A. D.; Strain, M. C.; Farkas, O.; Malick, D. K.; Rabuck, A. D.; Raghavachari, K.; Foresman, J. B.; Ortiz, J. V.; Cui, Q.; Baboul, A. G.; Clifford, S.; Cioslowski, J.; Stefanov, B. B.; Liu, G.; Liashenko, A.; Piskorz, P.; Komaromi, I.; Martin, R. L.; Fox, D. J.; Keith, T.; Al-Laham, M. A.; Peng, C. Y.; Nanayakkara, A.; Challacombe, M.; Gill, P. M. W.; Johnson, B.; Chen, W.; Wong, M. W.; Gonzalez, C.; Pople, J. A. *Gaussian 03*, revision B.05; Gaussian, Inc.: Wallingford, CT, 2004.

(13) (a) Weinhold, F.; Landis, C. R. *Valency and Bonding*; Cambridge University Press: Cambridge, 2005. (b) Glendening, E. D.; Badenhoop, J. K.; Reed, A. E.; Carpenter, J. E.; Bohmann, J. A.; Morales, C. M.; Weinhold, F. *NBO*, version 5.0; Theoretical Chemistry Institute, University of Wisconsin, Madison, WI, 2001.

(14) (a) Bader, R. F. W. *Atoms in Molecules: A Quantum Theory*; Clarendon Press: Oxford, U. K., 1990. (b) AIM 2000: A Program to Analyze and Visualize Atoms in Molecules. http://www.aim2000.de/.

(15) (a) Wight, C. A.; Ault, B. S.; Andrews, L. *J. Chem. Phys.* **1976**, *65*, 1244. (b) Andrews, L.; Ault, B. S.; Grzybowski, J. M.; Allen, R. O. *J. Chem. Phys.* **1975**, *62*, 2461.

(16) (a) Huber, K. P.; Herzberg, G. *Constants of Diatomic Molecules*; Van Nostrand Reinhold: New York, 1979. (b) Barnes, M.; Merer, A. J.; Metha, G. F. *J. Mol. Spectrosc.* **1997**, *181*, 180.